Materials Science and Engineering B 171 (2010) 127–132

Contents lists available at ScienceDirect

Materials Science and Engineering B

journal homepage: www.elsevier.com/locate/mseb

Relaxation dynamics of the conductive processes in $BaTiO_3$ ceramics at high temperature

Y. Leyet [a,*], F. Guerrero [a], J. Pérez de la Cruz [b]

[a] Departamento de Física, Facultad de Ciencias Naturales. Universidad de Oriente, Santiago de Cuba, C.P. 90500, Cuba
[b] INESCPorto, Rua do Campo Alegre, 687, 4169-007, Porto, Portugal

ARTICLE INFO

Article history:
Received 25 November 2009
Received in revised form 24 March 2010
Accepted 31 March 2010

Keywords:
$BaTiO_3$ ferroelectric ceramics
Conductive relaxation process
Dielectric anomaly

ABSTRACT

The temperature and frequency dependences of the undoped $BaTiO_3$ ceramics dielectric properties were measured between 25 °C and 700 °C and 100 Hz to 10 MHz, respectively. A dielectric anomaly was observed at low frequencies in the temperature range of 400–700 °C. This anomaly was associated to a low frequency dispersion process taking place at high temperature. The relaxation dynamics of the conductive process in $BaTiO_3$ ceramics was investigated. A relaxation function in the time domain ($\Phi(t)$) was determined from the frequency dependence of the dielectric modulus, using a relaxation function in the frequency domain ($F^*(\omega)$). In $BaTiO_3$ ceramics context, the best relaxation functions ($F^*(\omega)$), in the temperature ranges of 220–400 °C and 425 °C and 630 °C, were found to be a Cole–Cole and Davidson–Cole distribution functions, respectively. The relaxation function ($f(t)$) obtained by the time domain method was found to be a Kohlrausch–Williams–Watts (KWW) function type. The activation energy values (0.72 eV and 0.8 eV) reveal a mechanism correlated with the movement of single ionized oxygen vacancies and electrons of the second level of ionization, probably due to the formation of a titanium liquid phase during the sintering process.

1. Introduction

Barium titanate ($BaTiO_3$ or BT) ferroelectric system is a well-known ferroelectric and piezoelectric material below the Curie temperature $T_C \approx 120$ °C [1,2] and above this temperature it is cubic and paraelectric [2]. This material is mainly used as a dielectric multilayer ceramic capacitors, due to its high dielectric constant (1000–5000, depending on the grain size) and low losses. Other applications include: piezoelectric devices (such as: underwater transducers), resistors with positive temperature coefficient of resistivity (PTCR), electroluminescent panels, and embedded capacitance in printed circuit boards [1–3].

Some of the perovskite-type ferroelectric oxide materials, such as: $BaTiO_3$, show a diffuse dielectric anomaly in the temperature range of 700–1000 K [4–11]. Different origins have been associated to this dielectric anomaly (or relaxation process), however, it is not well explained yet. Bidault et al. [7] have collected information for several types of perovskite oxides, in order to clarify if the diffuse dielectric anomaly observed in these materials is an intrinsic or an extrinsic phenomenon. Although, they experimentally reported that in perovskite-type ferroelectric oxides the activation energy of dielectric relaxation in the diffuse dielectric anomaly is quantitatively similar to the conductivity activation energy of the sample, they did not give a definitive explanation.

On the other hand, combined effects of bulk and surface electrical properties [4,5] have been closely associated to the oxygen vacancies [4–6]. Recently, it was reported that this anomaly is a common feature of perovskite structures containing titanium, where the dielectric relaxation takes place due to the thermal motion of the oxygen vacancies [3].

The extrinsic nature of the diffuse dielectric anomaly in several ferroelectric materials, such as: $BaTiO_3$, and $Pb_{0.9}La_{0.1}TiO_3$ single crystals was confirmed experimentally by Choi et al. [12]. They also found that the diffuse dielectric anomaly is a competitive phenomenon between both the dielectric relaxation and the electrical conduction of the relaxing species, which are extrinsically formed in the lattice.

Taking into account the above mentioned considerations, it is possible to identify the parameters that provide information about the mechanisms that cause this anomaly. Parameters, such as: activation energy, dc conductivity, relaxation time, etc., determined by distribution functions in frequency domains, can be used to obtain information about the diffuse dielectric anomaly in pure $BaTiO_3$ ceramics. Generally, this dielectric behavior has been studied by distribution functions or Debye's model modified [7–9,11].

The aim of this work is to investigate, in details, the conduction mechanism of $BaTiO_3$ ferroelectric ceramics in wide temperature and frequency ranges, based on an analytical method that does not

* Corresponding author.
E-mail addresses: yuri@cnt.uo.edu.cu, yurileyet@yahoo.es (Y. Leyet).

0921-5107/$ – see front matter © 2010 Elsevier B.V. All rights reserved.
doi:10.1016/j.mseb.2010.03.085

require the calculation of the Fourier transforms. Moreover, the relaxation dynamics of the conductive process will be investigated using a temporal distribution function, which can be obtained by the dielectric modulus formalism.

2. Experimental procedure

A polymeric synthesis method [13], already used in the synthesis of nanosized powders and homogeneous ferroelectric ceramics, was used for the preparation of the $BaTiO_3$ ceramics. For this purpose, high purity precursors materials, such as: barium acetate ($BaC_4H_6O_4$, 99.9% – Synth), titanium tetra-isopropoxide ($Ti[OCH(CH_3)_2]_4$, 97% – Alfa Aesar), glycol-ethylene ($HOCH_2CH_2OH$, 97.78% – Synth), nitric acid (HNO_3, 65% – Dinamica) and citric acid ($C_6H_8O_7$, 99.5% – Synth), were used. Barium acetate was dissolved in citric acid in a molar ratio (1:4) and heated at 80 °C during 1 h. Titanium tetra-isopropoxide was dissolved in citric acid under the same above mentioned conditions, and afterward mixed, keeping constant (1:1) the Ba:Ti molar ratio. In order to form the polymeric chain ethylene-glycol was added to the BT solutions in a 2:3 molar ratio.

The resulting solutions were heated at 80 °C and spun constantly during 2 h, until a clear and transparent yellow solution was obtained. This process was maintained until a solidified dark brown glassy resin results, without any visible precipitation formation. The resins were heated at 5 °C/min up to 600 °C follow by a calcination process in air atmosphere at 600 °C during 5 h. The calcinated (pre-sintering) powders were palletized by uniaxial cold pressing. Afterward, the green pellet samples were sintered at 1275 °C during 2 h. Details of the preparation of this material have been reported elsewhere [14].

The dielectric characterization was carried out by an HP-4194A Impedance Gain Phase Analyzer over wide temperature and frequency ranges (25–650 °C and 20 Hz to 10 MHz, respectively).

3. Results and discussion

Fig. 1 shows the temperature dependence of the dielectric constant (ε'). In order to describe the temperature regions conveniently, there were denote two regions: (I) between 25 °C and 220 °C, corresponding to the phase transition ferroelectric-paraelectric region ($T_C \sim 130$ °C) and (II) between 220 °C and 650 °C, corresponding to the high temperature region, where the dielectric anomaly is observed. This anomaly is quite wide, with strong frequency dependence and a shift in the maximum temperature, typical characteristics of a relaxor process.

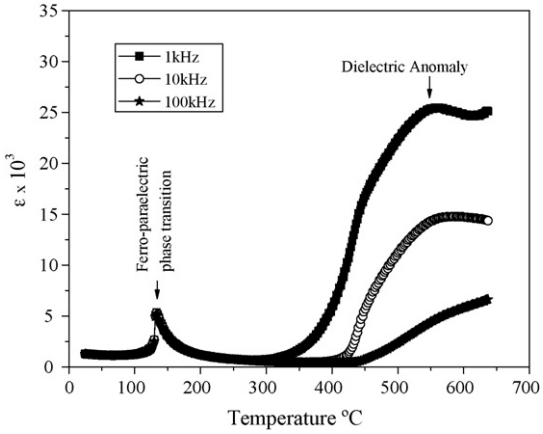

Fig. 1. Dielectric constant (ε') temperature dependence at different frequencies.

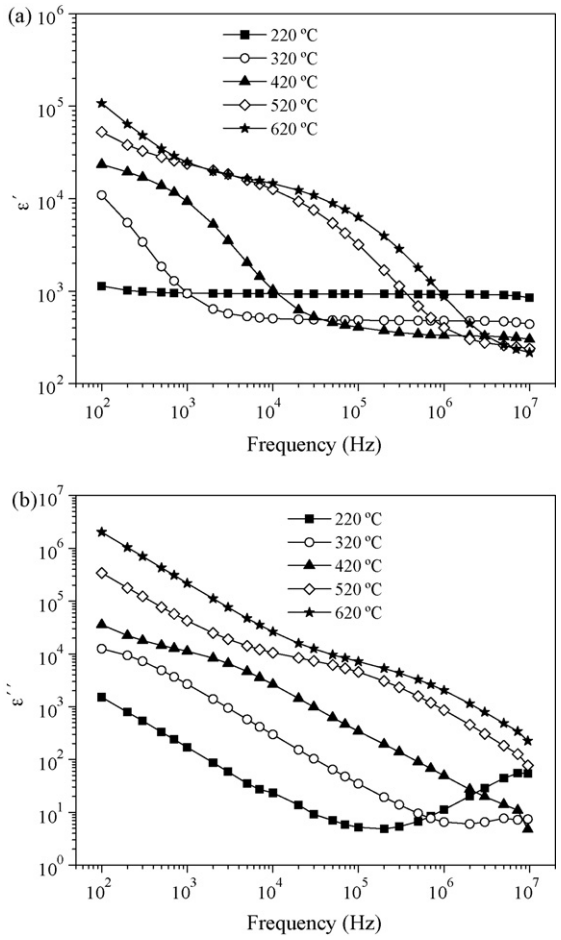

Fig. 2. Frequency dependence of (a) real (ε') and (b) imaginary (ε'') components of the dielectric permittivity at different temperatures.

Fig. 2 shows the frequency dependence of the real (ε') and imaginary (ε'') parts of the dielectric permittivity. The real part of the permittivity shows a classic dielectric material behavior in region I (dielectric permittivity constant up to 220 °C), as shown in Fig. 2(a). However, above this temperature (220 °C) the dielectric response changes to a typical relaxor behavior, as the temperature increases (region II). Fig. 2(b) shows low frequency dispersion up to 10 KHz, which have been associated with a conductive process due to point defects in the crystalline lattice [9,11]. It is also observed an increase in the values of ε' and ε'' as the temperature increase, which suggests the presence of a thermally activated process.

This fact have been explained based on the presence of oxygen vacancies that are created in the material during the sintering process; since, the BT formation require sintering temperatures higher than 1200 °C. In order to decrease the number of oxygen vacancies a very slow cooling process has been carried out, allowing the grains re-oxygenation through both material surface and grain boundaries. Nevertheless, it is always difficult to obtain oxygen vacancies free materials, which under the action of the temperature and a small electric field acquire enough energy to convert their self into charge carriers, and as a consequence form part of the conduction process [3].

The complex dielectric modulus ($M^* = 1/\varepsilon^*$) can be obtained from the temperature dependence of the real, ε', and imaginary, ε'', components of the dielectric permittivity ($\varepsilon^* = \varepsilon' - j\varepsilon''$). The M^* is one of the most appropriate formalisms for the investigation of conductive relaxation processes in many materials, fundamentally

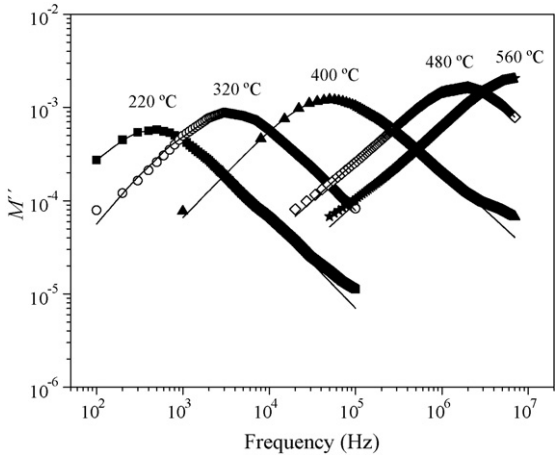

Fig. 3. Frequency dependence of the imaginary component of the dielectric modulus for BTceramics. The solid lines represent the CC and DC fitting curves in the temperature range selected (240 °C, 320 °C, 400 °C, 480 °C and 560 °C).

in ionic conductors [15], through the following equation:

$$M*(\omega) = M_{\infty}(1 - F*(\omega)) \quad (1)$$

where $M^*(\omega)$ is the complex electric modulus, M_∞ is the electric modulus at $\omega \to \infty$ and $F^*(\omega)$ is a relaxation distribution function in the frequency domain.

Fig. 3 shows the frequency dependence of the imaginary component (M'') at different temperatures. The evidence of the relaxation process, characterized by a frequency shift towards higher values with the increase of the temperature, is shown in this figure. Moreover, the maximum value of M'' remains practically constant as the working temperature increase, similar to the observed in some ionic conductors [16,17].

The analysis of the curves reveals two regions. The first region is observed between 220 °C and 440 °C and corresponds to a Cole–Cole (CC) relaxation distribution function: $F*_{CC}(\omega) = 1/1 + (i\omega\tau_{CC})^{\alpha}$, where τ_{CC} is the characteristic relaxation time and α is empiric parameter, that is between 0 and 1. Meanwhile, the second region (460–620 °C) is described by a Davison–Cole (DC) relaxation distribution function: $F*_{DC}(\omega) = 1/(1 + i\omega\tau_{DC})^{\gamma_{DC}}$, where τ_{DC} is the characteristic relaxation time and γ_{DC} is a empiric parameter, that is between 0 and 1. Both relaxation distributions functions were established from statistical parameters, with a correlation coefficient (R^2) of 0.99. This result could be associated with a conductive process of different mechanisms.

The normalized frequency dependence of the normalized imaginary dielectric modulus is shown in Fig. 4 (M''/M_m'' and f/f_m, where M_m and f_m are the maximum imaginary dielectric modulus and its respective frequency, respectively). As can be observed, in the temperature range of 220–620 °C all curves are overlapped, indicating that both mechanisms are independent of the temperature.

The study of the dynamics of a conduction process could be also carried out in the time domain [17]. In order to describe the temporal response of these distribution functions, it is common to use an analytical distribution function of relaxation times [17–19], which can be obtained using the relaxation parameters (τ, α and γ) in the frequency domain [17].

In the first region (220–440 °C), characterized by a CC distribution function, the Fourier transform for CC distribution function has been not establishments yet, being common to describe the temporal response using the analytical distribution function of the relaxation time [17–19], which can be expressed in the following

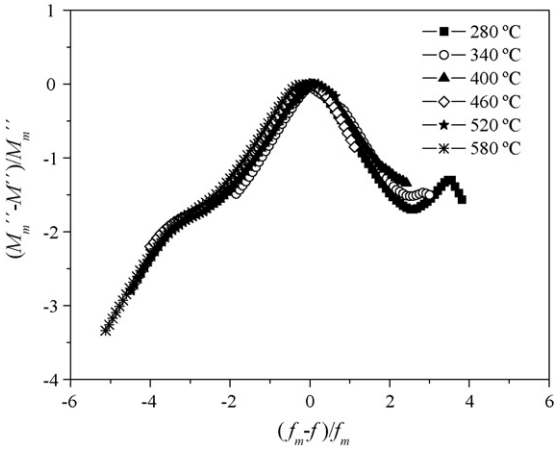

Fig. 4. Normalized frequency dependence (f/fm) of the imaginary component of the dielectric modulus (M''/Mm$''$) for BT ceramics, in the 220–630 °C temperature range.

form:

$$g_{CC} = \frac{1}{2\pi} \frac{\sin(\alpha\pi)}{\cos h[\alpha \ln(\tau/\tau_{CC}) + \cos(\alpha\pi)]} \quad (2)$$

The relaxation distribution function, in the time domain, can be obtained from the analytical function distribution (Eq. (2)) and can be expressed by Eq. (3) [17–19].

$$\Phi(t) = \int_0^{\infty} g_{CC}(\ln \tau) e^{-t/\tau} d \ln \tau \quad (3)$$

In the second region (460–620 °C) (where the distribution function corresponds to a DC-type function) the analytical distribution function in the frequency domain is given by [17]:

$$\Phi\bullet(t)_{DC} = \frac{1}{\Gamma(\gamma_{DC})\tau_{DC}} \left(\frac{t}{\tau_{DC}}\right)^{\gamma_{DC}-1} e^{-t/\tau_{DC}} \quad (4)$$

where $\Phi\bullet(t)_{DC}$ is the $\Phi(t)_{DC}$ derivate, $\Gamma(\gamma_{DC})$ is the Euler's gamma function evaluated in the γ_{DC} relaxation parameter, τ_{DC} is the relaxation time corresponding to DC relaxation function in the frequency domain.

The dependence of the relaxation distribution function $\Phi(t)$ with the logarithm of the time for six values of temperature (as an example), is shown in Fig. 5. In the first temperature region, $\Phi(t)$ remains almost independent of time until 10^{-5} s; while, at times higher than 10^{-5} s, the $\Phi(t)$ function decreases suddenly with the increase of the time, remaining practically constant again below

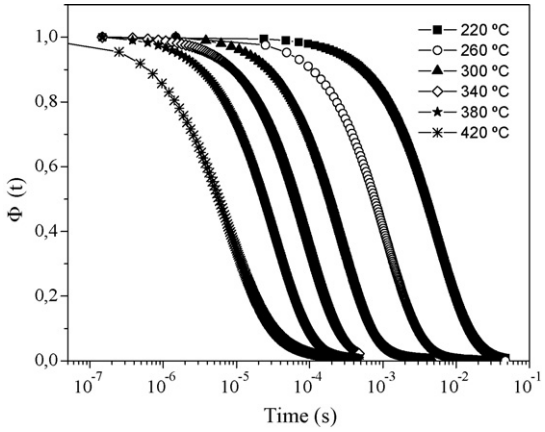

Fig. 5. Time dependence of the distribution function $\Phi(t)$ in the 220–420 °C temperature range. The solid lines represent the fitting with the KWW relaxation function in the time domain.

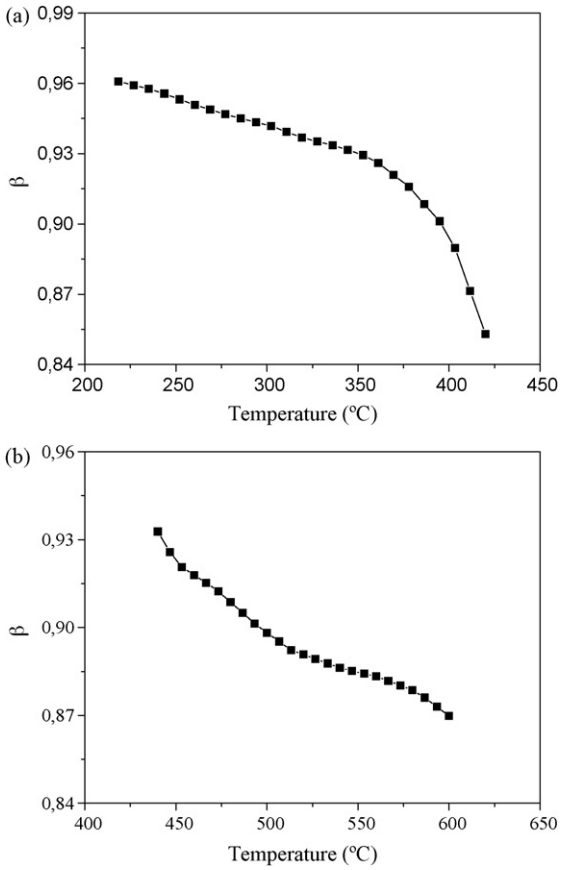

Fig. 6. Temperature dependence of the β parameter for BT ceramic sinterized at 1275 °C for 2 h. (a) 220–400 °C temperature range and (b) 420–600 °C temperature range.

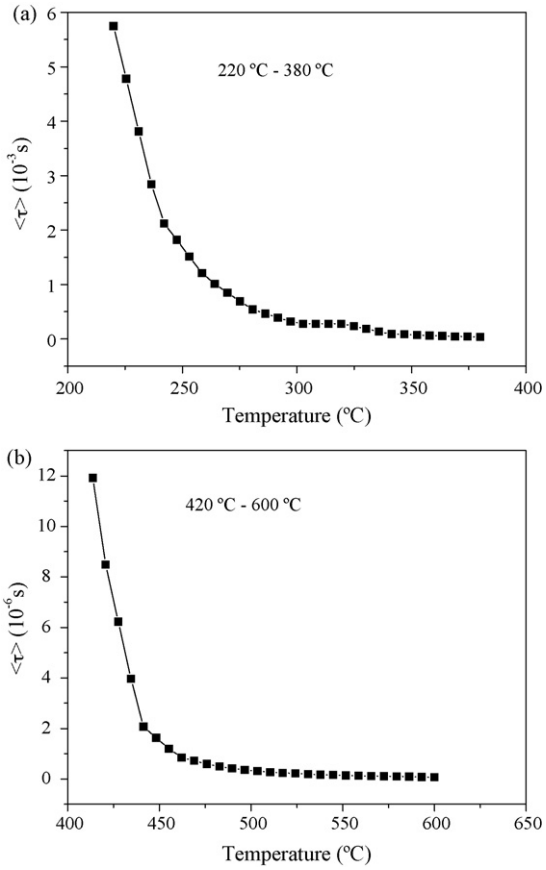

Fig. 7. Temperature dependence of the average relaxation time ($\langle\tau\rangle$) for BT ceramic sinterized at 1275 °C for 2 h. (a) 220–400 °C temperature range and (b) 420–600 °C temperature range.

5×10^{-3} s. On the other hand, in the second temperature region the relaxation function $\Phi(t)$ remains constant until $\sim 5 \times 10^{-4}$ s. After that, the $\Phi(t)$ curves fall abruptly to ~0. Moreover, there is a shift in the $\Phi(t)$ curves to higher temperature values (from 10^{-2} s to 10^{-1} s), as the working temperature is increased.

In order to analyze the resulting behavior, it is necessary to investigate the thermal evolution of the parameters of the relaxation distribution function, which can be obtained from the fitting of the distribution functions, as reported in the literature [17,18]. Among them, the Kohlrausch–Williams–Watts (KWW) function, expressed by the Eq. (5), was found to be the best adjustment distribution function.

$$f(t) = e^{-(t/\tau*)\beta} \tag{5}$$

This function in the time domain is normally known as 'stretched exponential', where the β and τ^* are the exponents that characterize the deformation and the characteristic relaxation time of the $f(t)$ function, respectively [16]. When the values of β are near to 0, a strong correlation exists between the hopping ion (relaxing ion) and its neighboring ions. Based on the τ^* and β values involved in Eq. (5), it is possible to determine the average relaxation times $\langle\tau\rangle$ from Eq. (6), where Γ is Euler's gamma function [15].

$$\langle\tau\rangle = \frac{\Gamma(1/\beta)}{\beta}\tau* \tag{6}$$

Fig. 6 shows the temperature dependence of the β parameter, which characterizes the relaxation process in the time domain. In Fig. 6(a), a slight decrease in the β values is observed with the increase of the temperature up to 350 °C. Afterwards a sudden fall in the β parameter takes place at 375 °C and 450 °C, indicating an increase in the correlation between the charge carrier and its vicinity. An inverse analysis (from 425 °C to 200 °C) shows an increase of β values until 0.93, which indicates a decrease in the correlation between the charge carriers and its vicinity and a change of the possible conductive mechanisms (associated with the change of the distribution functions) as the temperature decrease. At higher temperatures (region II), a new decrease of β is observed (see Fig. 6(b)). This behavior of β could be associated to an ions interchange process that occurs among the different planes of the crystalline lattice, suggesting a regimen where the interactions between the charge carriers should be reduced as the temperature is increased. It could be explained due to the start of conduction processes among the planes in the structure, and hence to a higher three-dimensional movement of the mobile ions. Rivera-Calzada et al. [20] have also reported a similar result in the LLTO system by using a RMN technique.

With the β and τ^* parameters obtained from the fitting of the $f(t)$ curves, it is possible to calculate the average relaxation time, which is associated to the ions jumping time (average delay of time spent by the ions to 'jump' from one site to another following a conduction path [19]). Fig. 7 shows the dependence of $\langle\tau\rangle$ with temperature in the BT ceramic. It is observed a rapid decreases in the $\langle\tau\rangle$ values, from 6.0×10^{-3} s to 1.5×10^{-5} s in the temperature range of 220–400 °C and from 1.5×10^{-5} s to 1.0×10^{-6} s in the temperature range of 425–630 °C, respectively. This exponential decrease of the $\langle\tau\rangle$ values indicates the presence of a thermally activated process, similar to the conductive process observed in ionic conductors [15].

The dc conductivity (σ_0) was determined based on the Eq. (7) and taking into account the equivalence between the frequency and

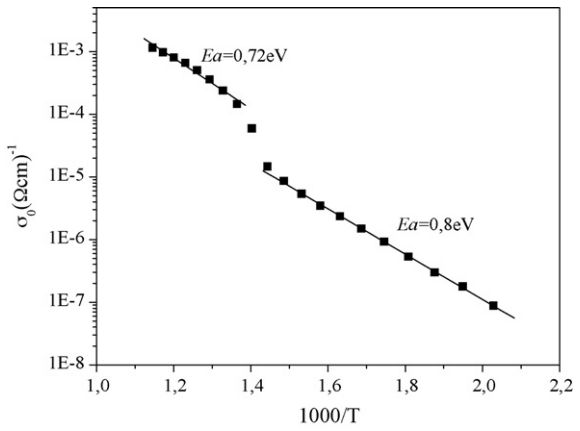

Fig. 8. The dependence of the dc conductivity as function of the inverse of the temperature and the activation energy values for the BT ceramic sinterized at 1275 °C for 2 h.

time domains.

$$\sigma_0 = \frac{\varepsilon_\infty}{\langle\tau\rangle} \tag{7}$$

where ε_∞ is the $\varepsilon(\omega)$ at $\omega \to \infty$.

The mechanism that causes the dc conductivity in the ferroelectrics material, in the low frequency and high temperature region, can be explained by the percolation model applied to the charge carrier diffusion. Considering that, the crystallographic sites associated with the moving of the ions are empties (participating in the ionic diffusion) and the rest of the crystallographic sites are occupied (blocking the diffusion of the moving ions); then, we can expect the formation of a cubic crystalline lattice of atomic positions, where the material stoichiometric is defined by the atomic positions blocked. On the other hand, the empties atomic positions are packing randomly, forming conduction lines and allowing the motion of the ions through the crystalline structure [20].

The temperature dependence of the dc conductivity is shown in Fig. 8. There are two regions, which follow the Arrhenius relation over the wide temperature range analyzed. This fact is associated with the two local conduction mechanisms and described by different distribution functions. These relatively high conductivity values can be associated with the existence of oxygen vacancies in the material, due to the electrical compensation in the crystalline lattice, caused by the Ti liquid phase formation during the preparation process. The above mentioned is the main source of the conduction by oxygen vacancies.

It is known that in perovskite structure materials containing titanate, the ionization of the oxygen vacancy will create the conducting electrons, rewritten as:

$$V_0 \leftrightarrow V_0^{\bullet} + e' \tag{8}$$

$$V_0^{\bullet} \leftrightarrow V_0^{\bullet\bullet} + e'' \tag{9}$$

or these electrons might be bonded to Ti^{4+} in the form of

$$Ti^{4+} + e' \leftrightarrow Ti^{3+} \tag{10}$$

Nevertheless, it is difficult to determine whether the weakly bonded electrons are located, near V_0 or near Ti ions [8]. The exact location of the electrons depends on the shape of the structure, temperature range, etc. Nevertheless, it has been shown that the oxygen vacancies lead to superficial electron levels. These electrons may be trapped by Ti^{4+} ions or oxygen vacancies, which can be easily activated thermally, becoming conducting electrons. The aforesaid fact indicates that there is close correlation among the oxygen vacancies, the electrons, and the dielectric relaxation process.

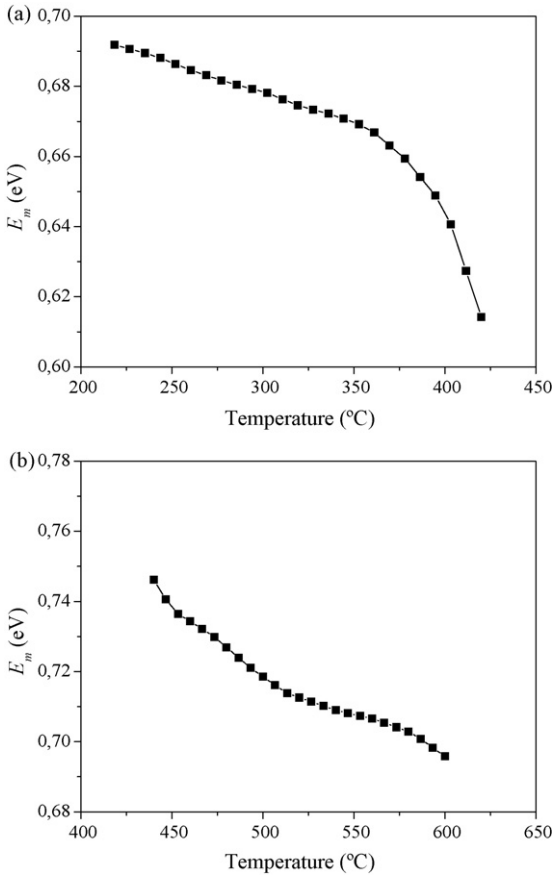

Fig. 9. Temperature dependence of the E_m for the BT ceramic sinterized at 1275 °C for 2 h. (a) 220–400 °C temperature range, (b) 420–600 °C temperature range.

The macroscopic activation energy values (E_a) are also shown in Fig. 8. The dc conductivity increases and the E_a decrease as the temperature increases, corroborating that the conductivity relaxation process is a thermally activated process.

It has been reported in the literature that the activation energy of the double ionized oxygen vacancies $V_0^{\bullet\bullet}$ is around 1.4 eV [8]. Moreover, if the electrical conductivity is governed by the thermal excitation of the charge carriers of single ionized oxygen vacancies, activation energy of ~0.7 eV could be obtained [8]. The activation energies reported in this work ($E_\sigma = 0.72 \pm 0.01$ and 0.8 ± 0.03 eV), indicate the existence of two conduction mechanisms. The first one, where the charge carriers responsible by the conduction are the single ionized oxygen vacancies, and the second mechanism, caused by the combination of single ionized oxygen vacancies with electrons of the second ionization state of the oxygen vacancies [8].

The resulting relaxation time (τ^*) activation energy is similar to the dc conductivity activation energy (E_σ). This activation energy represents the potential barrier that should be exceeded by the ions during the long-range conduction process, resulting from the correlated movement of the ions. On the other hand, the activation energy associated with the jumping of the ions from a site to its vicinity is called short-range microscopic activation energy (E_m), and can be determined by the expression (11).

$$E_m = \beta E_\sigma \tag{11}$$

The temperature dependence of the E_m is shown in Fig. 9. It is observed that the short-range microscopic activation energy is lower than the dc conductivity activation energy ($E_m < E_\sigma$) for each region. Moreover, the $E_m(T)$ behavior is similar to the reported for $\beta(T)$. The higher values of the dc conductivity activation energy

could be explained based on the higher energy level that should be surpassed by the ions during their motion, which result from their mutual interaction.

4. Conclusions

The BT system shows a conductive relaxation process in the low frequencies-high temperatures region. In the 220–400 °C and 425–630 °C temperature ranges, Cole–Cole and Davidson–Cole distribution functions were found to be the best frequency domain relaxation functions, respectively. Meanwhile, KWW distribution function was found to be the best time domain relaxation function. The thermal evolution of the relaxation parameters reveals that there is the not influence on the paraelectric-ferroelectric phase transition and viceverse. The values of the activation energy ($E_a \approx 0.72$ eV and 0.8 eV) in the investigated temperature interval suggest the existence of two conductive relaxation mechanisms, corresponding to the movement of single ionized oxygen vacancies and the combination of single ionized oxygen vacancies and electrons of the oxygen vacancies second ionization state.

References

[1] A. Testino, M.T. Buscaglia, M. Viviani, V. Buscaglia, P. Nanni, J. Am. Ceram. Soc. 87 (2004) 79–83.
[2] A.J. Moulson, J.M. Herbert, Electroceramics, Chapman & Hall, London, 1990.
[3] B. Jaffe, W.R. Cook, H. Jaffe, Piezoelectric Ceramics, Academic Press, London, 1971.
[4] R. Stumpe, D. Wagner, D. Bauerle, Phys. Stat. Sol. A 75 (1983) 143–154.
[5] M. Kuwabara, K. Goda, K. Oshima, Phys. Rev. B 42 (1990) 10012–10015.
[6] X. Dai, Z. Li, X.Z. Xu, S.K. Chan, D.J. Lam, Ferroelectrics 135 (1992) 39–48.
[7] O. Bidault, P. Goux, M. Kchikech, M. Belkaoumi, M. Maglione, Phys. Rev. B 49 (1994) 7868–7873.
[8] C. Ang, Z. Yu, L.E. Cross, Phys. Rev. B 62 (2000) 228–236.
[9] V.V. Lemanov, E.P. Smirnova, A.V. Sotnikov, M. Weihnacht, Appl. Phys. Lett. 77 (2000) 4205–4207.
[10] Y.W. Cho, S.K. Choi, Y.M. Vysochanskii, J. Mater. Res. 16 (2001) 3317–3322.
[11] B.S. Kang, S.K. Choi, Solid State Commun. 121 (2002) 441–446.
[12] S.K. Choi, B.S. Kang, Y.W. Cho, Y.M. Vysochanskii, J. Electroceram. 13 (2004) 493–502.
[13] M.P. Pechini, U.S. Patent No. 3,330,697.
[14] Y. Leyet, L. Aguilera, A. Pérez-Rivero, F. Guerrero, M.I.B. Bernardi, Rev. Cub. Quim. 22 (2010) 35–41.
[15] C. Leon, M.L. Lucia, J. Santamaría, S.F. Quesada, Phys. Rev. B 57 (1998) 41–44.
[16] Y. Feldman, A. Puzenko, Y. Ryabov, Chem. Phys. 284 (2002) 139–168.
[17] R.L. González, Y. Leyet, F. Guerrero, J. de Los, S. Guerra, M. Venet, J.A. Eiras, J. Phys-Condens. Mater. 19 (2007), pp. 136218-1–12.
[18] J.S. Kin, T.K. Song, J. Phys. Soc. Japan 70 (2001) 3419–3423.
[19] G. Williams, D.K. Thomas, Phenomenological and Molecular Theories of Dielectric and Electrical Relaxation of Materials, Novocontrol-Application Note Dielectrics 3, Germany, 1998.
[20] A. Rivera-Calzada, K. Kaminski, C. Leon, M. Paluch, J. Phys. Chem. B 112 (2008) 3110–3114.